Journal of Physics B: Atomic, Molecular and Optical Physics

Delocalization and superfluidity of ultracold bosonic atoms in a ring lattice

To cite this article: Fernanda Pinheiro and A F R de Toledo Piza 2013 *J. Phys. B: At. Mol. Opt. Phys.* **46** 205303

J. Phys. B: At. Mol. Opt. Phys. **46** (2013) 205303 (10pp) doi:10.1088/0953-4075/46/20/205303

Delocalization and superfluidity of ultracold bosonic atoms in a ring lattice

Fernanda Pinheiro[1,2,3] **and A F R de Toledo Piza**[1]

[1] Institute of Physics, University of São Paulo, São Paulo, Brazil
[2] Department of Physics, Stockholm University, SE-106 91 Stockholm, Sweden
[3] NORDITA, KTH Royal Institute of Technology and Stockholm University, SE-106 91 Stockholm, Sweden

E-mail: fep@fysik.su.se

Received 15 May 2013, in final form 6 September 2013
Published 15 October 2013
Online at stacks.iop.org/JPhysB/46/205303

Abstract
Properties of bosonic atoms in small systems with a periodic quasi-one-dimensional circular toroidal lattice potential subjected to rotation are examined by performing the exact diagonalization in a truncated many-body space. The expansion of the many-body Hamiltonian is considered in terms of the first-band Bloch functions, and no assumption regarding restriction to nearest neighbour hopping (tight-binding approximation) is involved. A finite size version of the zero temperature phase diagrams of Fisher *et al* (1989 *Phys. Rev.* B **40** 546570) is obtained and the results, in remarkable quantitative correspondence with the results available for larger systems, discussed. Ground-state properties relating to superfluidity are examined in the context of two-fluid phenomenology. The basic tool, consisting of the intrinsic inertia associated with small rotation angular velocities in the lab frame, is used to obtain the ground state 'superfluid fractions' numerically. They are analytically associated with one-body, uniform solenoidal currents in the case of the adopted geometry. These currents are in general incoherent superpositions of contributions from each eigenstates of the associated reduced one-body densities, with the corresponding occupation numbers as weights. Full coherence occurs therefore only when only one eigenstate is occupied by all bosons. The obtained numerical values for the superfluid fractions remain small throughout the parameter region corresponding to the 'Mott insulator to superfluid' transition, and saturate at unity only as the lattice is completely smoothed out.

(Some figures may appear in colour only in the online journal)

1. Introduction

Following the amazing development of experimental techniques in the latest years, cold atom systems became the primary candidates for the study of many-body quantum phenomena. Mean-field aspects of condensation, for example, have been extensively investigated both at the experimental [1, 2] and theoretical [3–8] levels. Properties of the strongly correlated regime became accessible with the use of optical lattices, and the transition from Mott-insulator to superfluid was verified in the lab [9]: in the superfluid phase, the atoms are delocalized in the lattice in a state with long-range coherence, whereas in the insulator phase they are localized in the lattice sites, each of these, with a fixed number of atoms [9].

Fundamental aspects of superfluid behaviour relating to flux properties in systems of alkali gases are still a matter of active research. The rigorous theoretical proof of superfluidity in the Gross–Pitaevskii limit was established only in 2002 [10], in terms of a criteria based on inertia and two-fluid arguments. In the current experimental scenario, different setups which include effects of rotation of containers have been proposed [11, 12] and/or realized [13]. In particular, persistent flow in a toroidal trap [14] and frictionless flow on a 2D system subjected to a moving obstacle [15] were observed very recently. This highlights the importance of explicitly considering the coupling of the system with its moving boundaries. In fact, in the context of optical lattices, earlier works [16, 17] have already investigated superfluid

properties in terms of the response of the system to imposed phase twists within the Bose–Hubbard model. In these studies, however, 'the influence of the lattice potential itself on the superfluid flow' has been neglected, and it is not clear how inclusion of such influence affects the superfluid properties and relates to the transition from localized to delocalized bosons in the many-body ground state.

Motivated by this, we investigate here superfluidity properties in a weakly interacting Bose gas trapped in a rotating annular toroidal Kronig–Penney trap, which constitutes a simplification of the experimentally implemented optical lattices. In order to study superfluidity in terms of an inertial criterion, we consider an externally imposed rotation ('cranking') of the lattice. The result is a 'cranked' extension of the field Hamiltonian underlying the Bose–Hubbard model. This Hamiltonian is conveniently expanded in a single-particle basis of Bloch functions and single-particle energies, and all the required two-body matrix elements are explicitly calculated. In the calculations reported below, the single-particle basis is truncated to the first band only. However, within the bounds set by this limitation, this treatment effectively relaxes the constraints inherent to the tight-binding approximation which underlies the standard usage of the Bose–Hubbard model: the range of the tunnelling is not restricted to nearest neighbours, and interactions are no longer restricted to occur on site. It therefore includes nontrivial many-body effects stemming from the multi-mode treatment as e.g. cross-collisional induced effects [18].

In terms of the results of the numerical many-body diagonalization, one can then obtain superfluid fractions (in the sense of the two-fluid model) and associated currents. These results are compared with results obtained for a finite version of the zero temperature phase diagram [19] of the Mott-insulator to superfluid transition. And despite being a small system, to which the strict definition of phase transition does not apply, it still deploys 'precursor' features which can be related even quantitatively to those which have been both observed in real systems and supported by approximate computational results obtained for considerably larger systems. In this context, properties relating to condensation are also analysed. We apply the Penrose–Onsager [20] criteria, which considers the establishment of occupation dominance of one of the eigenstates of the reduced density matrix. In particular, it is seen that the closure of the Mott lobes happens for the same range of parameter values at which occupation dominance essentially attains its peak value, and that these changes evolve in a scale different from that associated with the overall changes of the superfluid fraction and superfluid current.

This paper is organized as follows: in section 2 we present the cranked version of the lattice model, whose ground-state properties are analysed in section 3 in terms of the zero-temperature phase diagrams. In sections 4 and 5, we discuss properties related, respectively, to superfluidity and condensation, and in section 6 we present our conclusions.

2. The cranked quasi-momentum Hamiltonian

2.1. Bose–Hubbard model

The many-body dynamics of cold bosonic atoms in external lattice potentials is strongly dominated by the two basic ingredients consisting of hopping and short range (repulsive) two-body interaction effects [21]. In a tight-binding regime hopping is dominated by nearest-neighbour processes and two-body effects are dominated by 'on-site' contributions only. These ingredients are combined in the Bose–Hubbard model Hamiltonian

$$H_{BH} = -J\sum_{\langle i,j\rangle}(\hat{a}_i^\dagger \hat{a}_j + \hat{a}_j^\dagger \hat{a}_i) + \frac{U}{2}\sum_i \hat{a}_i^\dagger \hat{a}_i^\dagger \hat{a}_i \hat{a}_i, \quad J, U > 0, \tag{1}$$

where the first sum is restricted to nearest neighbours $\langle i, j\rangle$ and the operator $\hat{a}_i$ ($\hat{a}_i^\dagger$) destroys (creates) a bosonic particle in site i. In order to connect this Hamiltonian involving 'sites' to a more basic description involving spatial coordinates, one associates the sites to amplitudes defined in terms of the first-band Wannier function, which is sufficiently well localized in space in the tight-binding regime. As is now well known, competition between localization, favoured by two-body repulsion, and delocalization, favoured by the hopping term leads to a quantum phase transition between a 'Mott insulator' phase and a 'superfluid' phase in the ground state as the relative importance of the two parameters J and U of the model is varied [9, 19].

Specializing now to the case of a finite, one-dimensional potential array consisting (for convenience) of an odd number of sites M with periodic boundary conditions (i.e., a ring-shaped one-dimensional array of sites), interesting symmetries become manifest by changing to the representation which diagonalizes the hopping term of the Hamiltonian (1). This is achieved by a (discrete) Fourier transform

$$\hat{A}_q \equiv \frac{1}{\sqrt{M}}\sum_{n=1}^{M} \mathrm{e}^{\frac{2\pi \mathrm{i}}{M}nq}\hat{a}_n, \tag{2}$$

where $q = -\frac{M-1}{2}, \ldots, 0, \ldots, \frac{M-1}{2}$. In terms of the new 'quasi-momentum' bosonic operators $\hat{A}_q, \hat{A}_q^\dagger$, the Hamiltonian reads

$$H_{BH} = -2J\sum_{q=-\frac{M-1}{2}}^{\frac{M-1}{2}} \cos\left(\frac{2\pi q}{M}\right)\hat{A}_q^\dagger \hat{A}_q + \frac{U}{2M}\sum_{q_j}\delta_M(q_1+q_2-q_3-q_4)\hat{A}_{q_4}^\dagger \hat{A}_{q_3}^\dagger \hat{A}_{q_2}\hat{A}_{q_1}, \tag{3}$$

where the $\delta_M(q)$ in the two-body term is the modular Kronecker delta, equal to one if q is an integer multiple of M and zero otherwise. It indicates 'modular' conservation of total quasi-momentum ($Q_T = \mathrm{mod}(\sum_q qn_q,\ M)$), i.e, with allowance for *Umklapp* processes. This in fact reduces many-body Hamiltonian matrices to block-diagonal form, each block being associated with a value of Q_T, which assume the same values of q. In particular, traces of the tight-binding assumption are manifest in this representation in the cosine law for the single-particle energies and in the single common value U/M for the two-body matrix elements.

2.2. Configuration space field theoretical model

Limitations of the tight-binding regime which are built into the Bose–Hubbard Hamiltonian can be lifted without substantially increasing eventual computational costs by first returning to a configuration space representation of the Hamiltonian. We do this by keeping the overall geometry consisting of a regular toroidal array with mean radius R and containing M angular domains separated by potential barriers, with a one-dimensional lattice constant given by $l_c = 2\pi R/M$. Furthermore, we assume an effective one-dimensional regime in which the transverse amplitude is independent of angle and effectively frozen in its ground state. In this context, the relevant Hamiltonian can be written in terms of angle dependent bosonic field operators $\hat{\psi}(\varphi)$, $\hat{\psi}^\dagger(\varphi)$ as [5, 6]

$$H = \int \mathrm{d}\varphi\ \hat{\psi}^\dagger(\varphi)\left[\left(-\frac{\hbar^2}{2mR^2}\frac{\mathrm{d}^2}{\mathrm{d}\varphi^2} + V_{\mathrm{latt}}(\varphi)\right) + \frac{\Lambda}{2}\hat{\psi}^\dagger(\varphi)\hat{\psi}(\varphi)\right]\hat{\psi}(\varphi), \tag{4}$$

in which m is the boson mass and $V_{\mathrm{latt}}(\varphi)$ is the external lattice potential, accounting both for tight transverse confinement and for the angular periodicity. The effective one-dimensional strength parameter Λ is related to the strength of the usual effective two-body contact interaction given in terms of the s-wave scattering length a, $\lambda = 4\pi\hbar^2 a/m$, as

$$\Lambda = \lambda \int \mathrm{d}^2 r_\perp\ |w_0(\vec{r}_\perp)|^4.$$

Here $w_0(\vec{r}_\perp)$ is the frozen transverse amplitude in the array. This is a nodeless, normalized, confining wavefunction which sets the scale for the transverse size of the toroidal trap, and thus also the proportionality constant relating the effective strength parameters λ and Λ.

Before re-establishing contact with the Bose–Hubbard form (3) of the Hamiltonian, we consider a further extension of the effective one-dimensional Hamiltonian (4) to include uniform rotation of the lattice with angular velocity ω around the axis of the toroidal structure. By transforming to the reference frame rotating with the lattice potential, the required effective Hamiltonian becomes

$$H_\omega = \int \mathrm{d}\varphi\ \hat{\psi}^\dagger(\varphi)\left[\frac{1}{2mR^2}\left(\frac{\hbar}{\mathrm{i}}\frac{\mathrm{d}}{\mathrm{d}\varphi} - m\omega R^2\right)^2 + V_{\mathrm{latt}}(\varphi) + \frac{\Lambda}{2}\hat{\psi}^\dagger(\varphi)\hat{\psi}(\varphi)\right]\hat{\psi}(\varphi). \tag{5}$$

This differs from equation (4) just by the replacement

$$l_z \equiv \frac{\hbar}{\mathrm{i}}\frac{\mathrm{d}}{\mathrm{d}\varphi} \longrightarrow (l_z - m\omega R^2) \equiv \left(\frac{\hbar}{\mathrm{i}}\frac{\mathrm{d}}{\mathrm{d}\varphi} - m\omega R^2\right). \tag{6}$$

One can now make contact with the Bose–Hubbard form (3) by representing H_ω in the (truncated) single particle basis consisting of the M (first band) Bloch functions $\{\phi_q^{(\omega)}(\varphi)\}$ which diagonalize its one-body part. Note that these functions are labelled by the quasi-momentum q and depend on the cranking angular velocity ω. This is done by expressing H_ω in terms of the bosonic operators

$$\hat{A}_q^{\dagger(\omega)} = \int \mathrm{d}\varphi\ \phi_q^{*(\omega)}(\varphi)\hat{\psi}_q^\dagger(\varphi) \quad \text{and}$$

$$\hat{A}_q^{(\omega)} = \int \mathrm{d}\varphi\ \phi_q^{(\omega)}(\varphi)\hat{\psi}_q(\varphi),$$

which leads to

$$H^{(\omega)} = \sum_{q=0}^{M-1} e_q^{(\omega)}\hat{A}_q^{(\omega)\dagger}\hat{A}_q^{(\omega)} + \frac{\Lambda}{2}\sum_{q_i} g_{\{q_i\}}^{(\omega)}\delta_M(q_3+q_4-q_1-q_2) \times \hat{A}_{q_1}^{(\omega)\dagger}\hat{A}_{q_2}^{(\omega)\dagger}\hat{A}_{q_3}^{(\omega)}\hat{A}_{q_4}^{(\omega)}. \tag{7}$$

Here, the $e_q^{(w)}$ are the (first band) single particle Bloch eigenvalues and the objects $g_{\{q_i\}}^{(\omega)} \equiv g_{q_1,q_2,q_3,q_4}^{(\omega)}$ are integrals over products of four Bloch functions which, together with the strength parameter Λ, constitute the required two-body matrix elements in the adopted single-particle basis. The single particle energies are now the Bloch eigenvalues which, as shown in continuation, have spacings consistent with the cosine rule of (3) in the tight-binding regime; the two body matrix elements may and indeed do increasingly show fluctuations as one leaves the extreme tight-binding limit.

Finally, it is worth mentioning explicitly that truncation of the single-particle basis to the first-band Bloch states, together with the modular conservation of total quasi-(angular)momentum in (7) implies that there are no mean field two-body effects, i.e. all two-body matrix elements involving just one-particle changes of state vanish. As a consequence, reduced one-body density matrices of non-degenerate stationary many-body states of (7) will be diagonal in this base, total quasi-momentum being then a good quantum number.

2.3. Numerical implementation

In order to implement the many-body model (7) numerically, we first adopt a schematic realization of the lattice potential in terms of the Kronig–Penney model with δ-function barriers

$$V_{\mathrm{latt}} \to \gamma \sum_{n=0}^{M-1} \delta\left(\varphi - \frac{2\pi}{M}(n+1)\right),$$

where γ is the strength parameter for the δ-function barriers. For this choice, Bloch functions are given as analytic expressions involving few numerical parameters which are easily obtained, together with the Bloch eigenvalues, by solving transcendent algebraic equations numerically.

The behaviour of the Bloch eigenvalues as a function of the cranking angular velocity ω, given in units of $\omega_0 = \hbar/mR^2$ (energy being measured in units of $\epsilon_0 \equiv \hbar^2/mR^2$), is shown for two values of the barrier parameter γ in figures 1(a) and (b). Part (c) of the same figure shows the ω dependence of the tight-binding regime one-body eigenvalues as implemented in the Bose–Hubbard model, given by the function $-2\cos\left(\frac{2\pi}{M}(q-\omega)\right)$ (cf equation (3)). While this cosine function is clearly capable of reproducing the relative spacings of the Bloch single-particle energies very accurately for sufficiently large values of γ, deviations from it are clearly seen in the case of the lower value of γ. We use single particle Bloch eigenvalues $e_q^{(w)}$ obtained numerically in all calculations, while taking

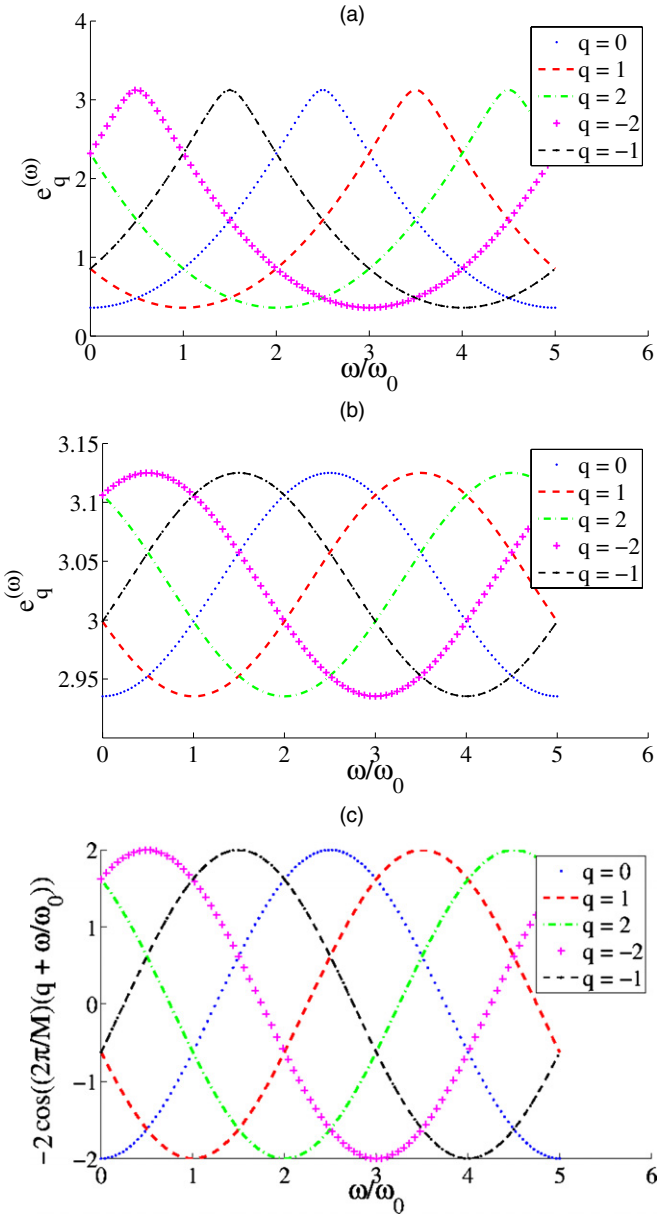

Figure 1. First-band Bloch single-particle energies (in units of $\epsilon_0 = \hbar^2/mR^2$), for $M = 5$, $\gamma = 1\epsilon_0$ (a) and $100\epsilon_0$ (b), as functions of the cranking angular velocity ω (in units of ω_0). (c): Bose–Hubbard single-particle energies per unit hopping parameter also as a function of ω. Note the distortion relative to the cosine law (c) in case (a). One quarter of the width of the Bloch band may be used as an effective Bose–Hubbard hopping parameter J for each value of γ, as discussed in the text. The values of J for (a) and (b) are 0.691 and 0.0474 respectively, also in units of ϵ_0.

advantage of the analytical expression valid in the tight-binding regime to *define* a parametrization of the barrier strength in terms of an effective hopping coefficient J as

$$J \equiv \frac{\epsilon_\gamma^> - \epsilon_\gamma^<}{4}. \tag{8}$$

Here, $\epsilon_\gamma^>$ and $\epsilon_\gamma^<$ are respectively the upper and the lower bounds for the first-band cranked Bloch eigenvalues $\{\epsilon_q^{(\omega)}\}$ for a given value of the barrier strength parameter γ. For simplicity, we refer to the numerator of equation (8) as the 'energy width of the first band'. This parametrization coincides

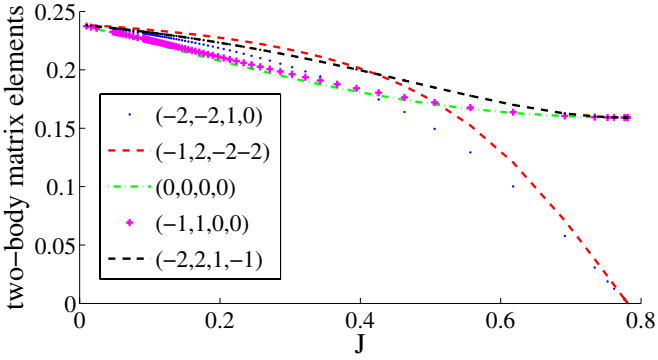

Figure 2. Typical behaviour of the two-body matrix elements. The notation (q_1, q_2, q_3, q_4) denotes the integral $\int d\varphi \phi^*_{q_1}(\varphi)\phi^*_{q_2}(\varphi)\phi_{q_3}(\varphi)\phi_{q_4}(\varphi)$. Unlike strictly quasi-momentum conserving matrix elements, *Umklapp* matrix elements vanish together with barrier strength parameter at $J = 25/32\epsilon_0 = 0.781\,25\epsilon_0$.

with the Bose–Hubbard definition of the hopping parameter in equations (1) and (3) in the tight-binding domain. Note also that the dependence of the Bloch energies with the cranking angular velocity leads to single-particle energy level crossings at integer and half-integer values of ω/ω_0. Since the quasi-momentum is a good quantum number for the individual Bloch states, these level crossings will have a decisive role in determining the total quasi-momentum of cranked many-body ground state, as discussed in the following section.

The four wavefunction integrals $g^{(\omega)}_{q_1,q_2,q_3,q_4}$ are easily evaluated in terms of the Bloch functions. Some sample results are shown in figure 2, for $M = 5$ and $\omega = 0$, as functions of the effective hopping parameter J just defined. Salient features here are the complete bunching on a single value g_0 in the tight-binding limit $J \to 0$ ($g_0 \sim 0.239$ in the present case), and the strong quenching of *Umklapp* matrix elements in the opposite limit of very large hopping, as compared to angular momentum conserving matrix elements. Note that definition (8) of the effective hopping parameter leads to $J/\epsilon_0 \to 25/32 = 0.781\,25$ as the barrier strength parameter $\gamma \to 0$, for the present case with $M = 5$. In order to facilitate comparison with results obtained using the Bose–Hubbard Hamiltonian parameters as in (1) and (3), we again use the tight-binding limit to *define* an effective two-body parameter U to replace the two-body constant Λ as

$$U \equiv g_0 M \Lambda \tag{9}$$

in terms of which the two-body part of equation (7) coincides in the tight-binding limit to that of the Bose–Hubbard model, equation (3).

3. The ground-state phase diagram

The different dynamical regimes prevailing in different parameter domains [19] of the Bose–Hubbard Hamiltonian (3) have been studied extensively using diverse approximation schemes and/or computational techniques. The focus of these studies is the thermodynamic limit, in which the number of sites and the number of bosons go to infinity at fixed finite mean occupation per site. The one-dimensional case has been treated

rather recently by Kühner*et al* [22], including, in particular, the 'ground-state phase diagram' [19] in which different phase domains are identified in a $\mu/U \times J/U$ diagram, μ being the chemical potential.

Our purpose in this section is to indicate how one can obtain phase-diagram information by using the results of exact many-body diagonalization of the Hamiltonian (7), albeit with feasibly small number of sites and of bosons. Under these circumstances, there will of course be no case for taking thermodynamic limits and determining precise phase boundaries, but as will be shown explicitly there are clear 'precursor features' in the small number solutions which clearly identify, surprisingly even quantitatively, several thermodynamic limit properties.

Since in this context we deal always with systems having a fixed, given number of particles, a replacement must be devised for the chemical potential μ. We thus replace μ by the addition energy Δ_N, N being the number of bosons, defined as $\Delta_N = E_0(N+1) - E_0(N) - \epsilon$, where $E_0(N)$ denotes the ground-state eigenvalue for N bosons in the chosen number of sites, and ϵ is the average of the single particle (first-band Bloch) energies. Note that ϵ vanishes for the cosine law of the Bose–Hubbard Hamiltonian (3). With this replacement, the axes of the graph corresponding to the ground-state phase diagram become

$$\frac{\mu}{U} \to \frac{\Delta_N}{U} = \frac{E_0(N+1) - E_0(N) - \epsilon}{U}, \quad \frac{J}{U} \tag{10}$$

where we use the quantities U and J as defined in equations (9) and (8) in order to characterize the dynamical parameters of the many-body Hamiltonian (7).

Results obtained for $M = 5$ sites and $N = 0$ to 11 bosons are shown in figure 3(a), for the usual situation of vanishing cranking angular velocity, $\omega = 0$, the strength of the two-body effective interaction having been fixed at $\Lambda = 0.06\epsilon_0$. This value is realistic in the sense that it corresponds to the mass and scattering length of ^{87}Rb for $R \sim 10$ μm with a transverse confinement scale of the order of 1 μm. The value of the barrier strength parameter γ has been varied to cover the desired range of values of J/U. Actually, the whole parameter domain covered by this graph falls within the tight-binding domain in which the results obtained using the Hamiltonian (7) differ very little from what one obtains using the Bose–Hubbard Hamiltonian (3) itself [24]. Each curve in this graph shows the dependence on J/U of the (U-scaled) addition energy Δ_N for one of the values of N. As seen, the bunching of these curves at integer values of the U-scaled addition energies in the limit $J/U \to 0$ gives room for the Mott insulator lobes. The shape and range of these lobes reproduces even quantitatively the results obtained towards the thermodynamic limit, cf [22], including in particular the 'reentrant behaviour' [23] (see also [25]) characteristic of the one-dimensional Bose–Hubbard model. Moreover, one can show perturbatively, in the large J/U limit past the insulator lobes, that the spacing between consecutive Δ_N/U curves approaches the value $1/M$, M being the number of sites [24], suggesting therefore a definite N-cleavage as one moves towards the thermodynamic limit.

Effects of cranking are illustrated in figure 3(b), which differs from (a) in that here $\omega = 0.48\omega_0$, i.e. just shortly

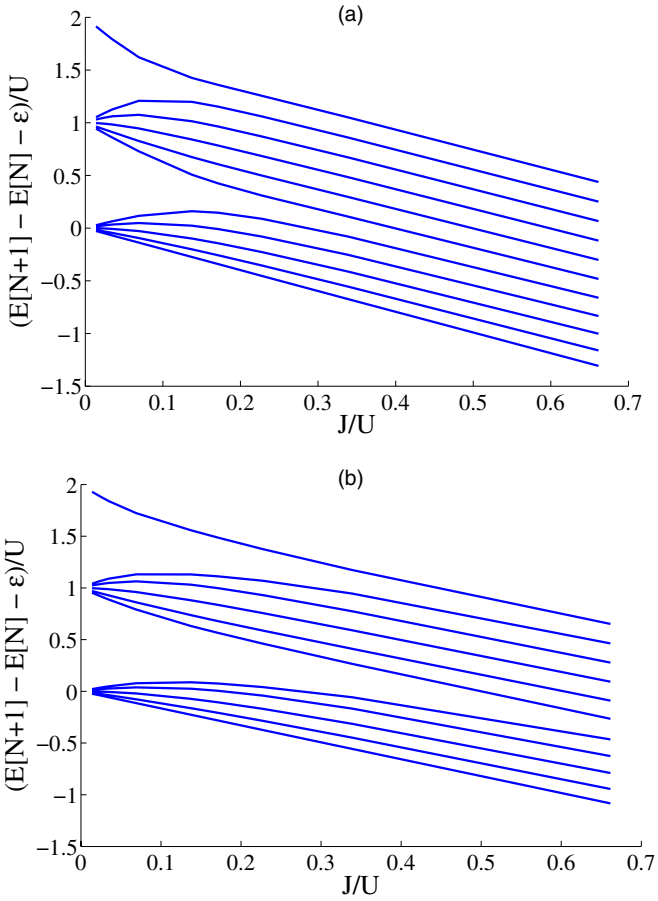

Figure 3. Scaled particle addition energies as functions of J/U for $\omega = 0$ and $\omega = 0.48\omega_0$ using (the) single-particle energies, and with the effective hopping parameter defined in the text. Here $\Lambda = 0.06\epsilon_0$, $M = 5$ and N varies from 0 to 11 (from the first to the last line going upwards). In (a), the closure of the lowest Mott lobe is seen to happen in the neighbourhood of $J/U \sim 0.35$, while in (b) it is affected by the angular velocity and happens for higher values, $J/U > 0.7$.

before the first single-particle level crossing (see figure 1). The broadening and lengthening of the Mott insulator lobes which is visible in this case is governed essentially by the Bloch energies modified by rotation. This effect can be understood in terms of the effective reduction of the kinetic energy (cf equation (6)) which quenches hopping thus favouring the insulating phase.

4. Properties related to superfluidity

The dependence on ω of the energy (in the rotating system) of the many-body ground state of the cranked Hamiltonian (3), for small values of the angular velocity, allows for the determination of an inertial parameter $\mathcal{I}$ through the relation

$$E^{(\omega)}(N) = E^{(0)}(N) + \frac{\mathcal{I}}{2}\omega^2 + \mathcal{O}(\omega^4), \quad \omega \to 0$$

which may be related to the 'superfluid fraction' f_s, defined within the phenomenological framework of the two-fluid model of superfluid behaviour, as (cf [4])

$$f_s = \frac{\mathcal{I}}{\mathcal{I}_{\mathrm{Rig}}} = \frac{\mathcal{I}}{NmR^2}, \tag{11}$$

where $\mathcal{I}_{\rm Rig} = NmR^2$ is the rigid moment of inertia of the system. This bears the understanding that, in stationary state, as viewed from the rotating frame, the inertia corresponds to that part of the fluid which remains stationary in the lab frame (the 'superfluid'), while the 'normal' component is carried around with the externally imposed angular velocity.

4.1. Current for inertial parameter

The inertial parameter $\mathcal{I}$ can be expressed as

$$\mathcal{I} = 2\frac{{\rm d}E^{(\omega)}(N)}{{\rm d}\omega^2}\bigg|_{\omega\to 0} = \frac{1}{\omega}\langle\Phi^{(\omega)}\left|\frac{{\rm d}H_\omega}{{\rm d}\omega}\right|\Phi^{(\omega)}\rangle\bigg|_{\omega\to 0} \tag{12}$$

where $|\Phi^{(\omega)}\rangle$ is the state vector for the N-body ground state at cranking angular velocity ω and where the well-known Feynman–Hellmann relation has been used. This last expression involves the expectation value of the derivative of H_ω, equation (5), with respect to the parameter ω. This derivative is in fact a one-body (albeit nonlocal) operator:

$$\frac{{\rm d}H_\omega}{{\rm d}\omega} = -\int {\rm d}\varphi\, \hat\psi^\dagger(\varphi)\left(\frac{\hbar}{\rm i}\frac{\rm d}{{\rm d}\varphi} - mR^2\omega\right)\hat\psi(\varphi). \tag{13}$$

All the information relevant for one-body observables, contained in the correlated many-body ground state $|\Phi_0^{(\omega)}\rangle$ of the Hamiltonian (7), is carried by its associated one body reduced density, defined as $\rho^{(1)}(\varphi,\varphi') \equiv \langle\Phi_0^{(\omega)}|\hat\psi^\dagger(\varphi')\hat\psi(\varphi)|\Phi_0^{(\omega)}\rangle$. We may thus proceed to express the inertial parameter $\mathcal{I}$, as given by equation (12), in terms of this object. For this purpose, it is convenient to use its spectral decomposition, which involves the solutions of the eigenvalue problem

$$\int {\rm d}\varphi'\rho^{(1)}(\varphi,\varphi')\chi_\nu(\varphi') = n_\nu\chi_\nu(\varphi)$$

where the single-particle eigenfunctions $\chi_\nu(\varphi)$ are the so called natural orbitals, the associated eigenvalues n_ν being the corresponding occupation numbers [26]. In terms of these ingredients, the one-body reduced density can be expressed as

$$\rho^{(1)}(\varphi,\varphi') = \sum_\nu n_\nu\chi_\nu(\varphi)\chi_\nu^*(\varphi'). \tag{14}$$

Using (13) and (14) in equation (12), one finds that the inertial parameter $\mathcal{I}$ can be written in the form

$$\mathcal{I} = \frac{mR^2}{\omega}\int {\rm d}\varphi\, j_\omega(\varphi)\bigg|_{\omega\to 0} \tag{15}$$

where the current $j_\omega(\varphi)$ is given by

$$j_\omega(\varphi) \equiv -\sum_\nu n_\nu\left[\frac{\hbar}{mR^2}{\rm Im}\left(\chi_\nu^*(\varphi)\frac{{\rm d}\chi_\nu}{{\rm d}\varphi}\right) - \omega|\chi_\nu(\varphi)|^2\right]. \tag{16}$$

To obtain this expression, matrix elements involving a φ-derivative have been evaluated with the prescription

$$\int {\rm d}\varphi\hat\psi^\dagger(\varphi)\frac{\rm d}{{\rm d}\varphi}\hat\psi(\varphi) = \int {\rm d}\varphi\int {\rm d}\varphi'\hat\psi^\dagger(\varphi)\delta'(\varphi-\varphi')\hat\psi(\varphi')$$

where $\delta'(\varphi)$ is the first derivative of the Dirac delta function with respect to the argument.

The current $j_\omega(\varphi)$ is therefore, in general, an incoherent sum of currents associated with each natural orbital, full coherence resulting only in the limiting case of full occupancy of a single natural orbital. Moreover, it is easy to see that the current $j_\omega(\varphi)$, together with the (diagonal part of the) one-body reduced density, obeys a conservation law which, for the stationary states of the cranked Hamiltonian (5), in fact makes it *independent of* φ (i.e., solenoidal) as a result of the time independence of the associated one-body reduced density.

In order to see this, we begin from the expression of the many-body Hamiltonian in terms of the field operators, equation (7), and use the stationary character of $|\Psi^{(\omega)}\rangle$

$$H_\omega|\Psi^{(\omega)}(t)\rangle = {\rm i}\hbar\frac{\rm d}{{\rm d}t}|\Psi^{(\omega)}(t)\rangle,$$
$$|\Psi(t)^{(\omega)}\rangle = {\rm e}^{-\frac{\rm i}{\hbar}E_0^{(\omega)}t}|\Phi^{(\omega)}\rangle$$

to write the vanishing time derivative of the reduced one-body density as

$$\frac{\rm d}{{\rm d}t}\rho(\varphi,\varphi')\,|_{\varphi=\varphi'} = \frac{\rm d}{{\rm d}t}\langle\Psi^{(\omega)}|\hat\psi^\dagger(\varphi)\hat\psi(\varphi')|\Psi^{(\omega)}\rangle\,|_{\varphi=\varphi'}$$
$$= \frac{1}{{\rm i}\hbar}\langle\Phi^{(\omega)}|[\hat\psi^\dagger(\varphi)\hat\psi(\varphi'), H_\omega]|\Phi^{(\omega)}\rangle\,|_{\varphi=\varphi'} = 0.$$

By computing the φ-derivatives with the prescription

$$\int {\rm d}\varphi\hat\psi^\dagger(\varphi)\frac{{\rm d}^2}{{\rm d}\varphi^2}\hat\psi(\varphi) =$$
$$= \int {\rm d}\varphi\int {\rm d}\varphi'\hat\psi^\dagger(\varphi)\delta''(\varphi-\varphi')\hat\psi(\varphi'),$$

where $\delta''(\varphi)$ stands for the second derivative of the Dirac delta function with respect to the argument, the commutator can again be expressed in terms of the reduced one-body density expressed in terms of its natural orbitals with the result

$$\frac{\rm d}{{\rm d}\varphi}\sum_\nu n_\nu\left[\frac{\hbar}{mR^2}{\rm Im}\left(\chi_\nu^*(\varphi)\frac{{\rm d}\chi_\nu(\varphi)}{{\rm d}\varphi}\right) - \omega|\chi_\nu(\varphi)|^2\right] = 0, \tag{17}$$

which states the φ independence of the current j_ω.

Using (17), the expression for the inertial parameter $\mathcal{I}$, equation (15), reduces to

$$\mathcal{I} = mR^2\frac{2\pi}{\omega}j_\omega\bigg|_{\omega\to 0}.$$

Correspondingly, the 'superfluid fraction' f_s is expressed in terms of this current as

$$f_s = \frac{1}{N}\frac{2\pi}{\omega}j_\omega\bigg|_{\omega\to 0}. \tag{18}$$

In fact, the last two factors clearly amount to the time integral of the solenoidal current j_ω for the duration of one period of the cranking.

A feature of the evaluation of superfluid fractions by means of equations (11) and (18) which is worth stressing is that the definition of the current j_ω stems directly from the inertial parameter $\mathcal{I}$, being identified as the expectation value of a momentum dependent one-body operator, and therefore apt to be expressed in terms of the one-body reduced density, independently of any assumptions concerning the relevance of a condensate wavefunction [16, 17]. This possibly manifests itself *a posteriori*, through the coherence properties of the current.

It is worth noting that the formal results (15)–(17) can be extended in a straightforward way to a more general context, involving stationary many-boson states in an arbitrary three-dimensional external trap, cranked around a fixed axis specified by the unit vector $\vec{u}$. The effective Hamiltonian (5) is in this case replaced by

$$H_\omega \to \int \mathrm{d}^3 r\, \hat{\psi}^\dagger(\vec{r}) \left[\frac{1}{2m} \left(\frac{\hbar}{\mathrm{i}} \vec{\nabla} - m\omega(\vec{u} \times \vec{r}) \right)^2 + V_{\mathrm{trap}}(\vec{r}) + \frac{\lambda}{2} \hat{\psi}^\dagger(\vec{r}) \hat{\psi}(\vec{r}) \right] \hat{\psi}(\vec{r}). \tag{19}$$

Following the procedure just described for the one-dimensional case, one obtains from (19) an expression for the inertial parameter that is given in terms of the volume integral of the appropriately weighted tangential component of a solenoidal current density. This current is again written as an incoherent sum of currents associated with the natural orbitals, and that are weighted by the corresponding occupation numbers.

4.2. Numerical results

For the case of the calculations reported here, the fact that the many-body states $|\Phi_0^{(\omega)}\rangle$ have good total quasi-momentum, together with the adopted truncation to single boson states of the first band only, ensures that the associated reduced one-body densities are diagonal in the quasi-momentum representation, i.e.

$$\langle \Psi_0^{(\omega)} | \hat{A}_q^{(\omega)\dagger} \hat{A}_{q'}^{(\omega)} | \Psi_0^{(\omega)} \rangle = n_q \delta_{qq'}. \tag{20}$$

The natural orbitals are thus just the Bloch functions $\phi_q^{(\omega)}$ themselves, so that the corresponding occupation numbers n_q may accordingly be labelled by the associated quasi-momentum q. As a numerical check, we evaluate the superfluid fraction f_s both by taking numerical derivatives of the ground-state eigenvalue $E^{(\omega)}(N)$ with respect to ω^2, as written in equation (12), and in terms of the current j_ω, as in equation (18), the current being evaluated as in equation (16), in terms of the Bloch functions and of the eigenvalues n_q of the reduced one-body density, equation (20). In order to deal with the implied limit $\omega \to 0$ in the numerical evaluation of superfluid fraction values from either equations (11) and (12) or from equation (18), we use the fact that the value obtained is very stable against variation of the value of ω. This remains true even by orders of magnitude down from $\omega \sim 0.1\omega_0$, as long as the differences involved in obtaining either $\mathcal{I}$ or j_ω are sufficiently above the limitations set by machine precision. In view of equation (15), this amounts to a numerical verification that the ω-dependence of $E^{(\omega)}(N) - E^{(0)}(N)$ is quadratic, while that of j_ω is linear within such a range.

Results for the commensurate case $N = M = 5$ are shown in figure 4, where the values obtained for the superfluid fraction f_s are plotted as a function of the hopping parameter J for two values of the two-body strength parameter Λ (or U, see equation (9)). The most striking result of the numerical evaluation of the superfluid fraction for the model system on hand is the 'prima facie' absence of any dramatic features in the parameter domain ($J \sim 0.025\epsilon_0$ for $\Lambda = 0.06\epsilon_o$ and $J \sim 0.125\epsilon_0$ for $\Lambda = 0.3\epsilon_0$) which supports the transition

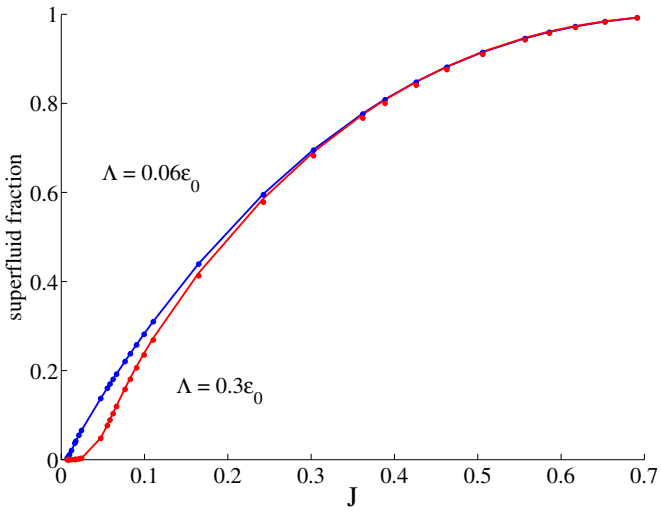

Figure 4. Superfluid fraction for the system with $N = M = 5$ and $\Lambda = 0.06\epsilon_0$ and $\Lambda = 0.3\epsilon_0$. The curves correspond to equations (11) and (12) while the points are obtained using the solenoidal current as in equation (18). See text for details.

associated with the closing of the Mott insulator lobes (cf figures 3(a) and 4). In fact, while being affected by the increase of the two-body interaction parameter, the superfluid fraction retains there a smooth monotonically increasing behaviour saturating at the full scale of the hopping parameter J.

Effects related to the presence of the Mott insulator lobes in the ground-state phase diagram of figure 3(a) do appear, however, in the corresponding intervals of J/U and consist of a quenching of the calculated superfluid fraction in such intervals at the corresponding commensurate filling, relative to the values obtained for incommensurate filling. This is shown in figures 5(a) and (b) for the cases $N/M = 1$ and 2, respectively. As discussed in section 5 below, fragmentation of the total boson number N over occupations n_q of different natural orbitals occurs in the J/U domains spanned by the Mott insulator lobes and is stronger in the case of commensurate occupation (see figures 6(a) and (d)). The quenching effect may thus be associated with stronger loss of coherence of the current j_ω (see equation (15)) for commensurate filling. Note that, for the 'realistic' value $\Lambda = 0.06\epsilon_0$ of the two body strength parameter, the calculated values of the superfluid fraction are small in the whole J/U domains associated with the Mott insulator lobes, so that these effects are not conspicuous on the scale used in figure 4.

A comment relating the results obtained for the superfluid fraction as understood in [17] is also in order. A connection to the present evaluation of superfluid fractions can in fact be established analytically in a rather straightforward way by noting that equation (12) can in particular be applied to an ideal gas ($U = 0$), in which case the ground state for small ω consists of the N bosons occupying the lowest ($q = 0$) quasi-momentum Bloch orbital. In the tight-binding approximation the ground-state energy is thus given by

$$E_{\mathrm{ideal}}^{(\omega)}(N) = -2JN \cos\left(\frac{2\pi\omega}{M\omega_0}\right), \quad \omega_0 = \frac{\hbar}{mR^2},$$

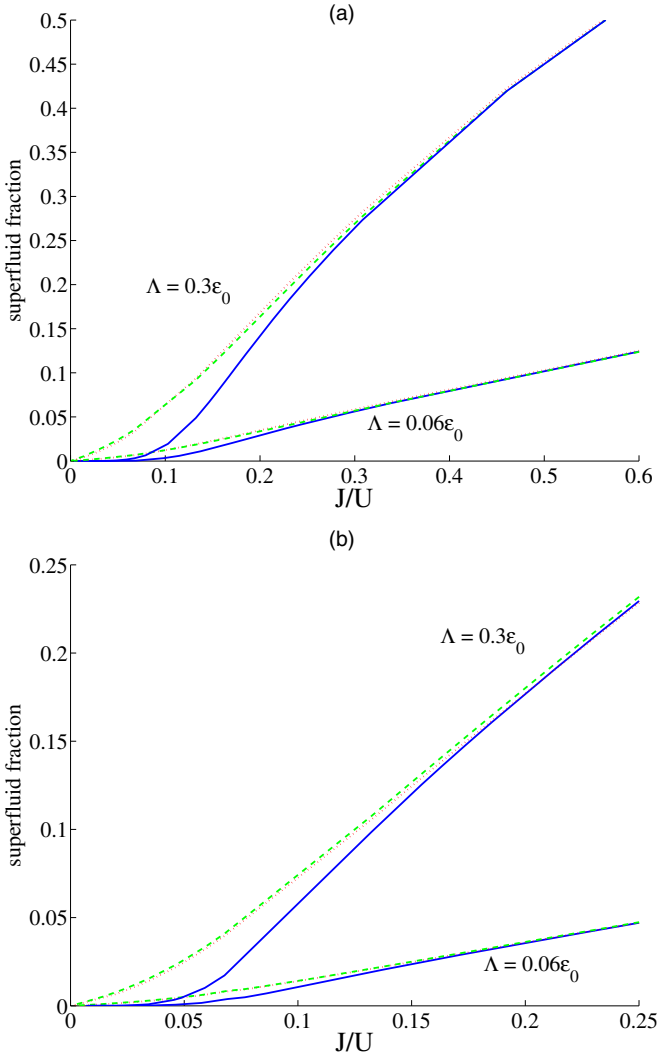

Figure 5. Quenching of the superfluid fraction at commensurate fillings, $N_1 = M$ in (a), $N_2 = 2M$ in (b). In both cases results are given for the two values $\Lambda = 0.06\epsilon_0$ and $\Lambda = 0.3\epsilon_0$ of the two body strength parameter. Curves for $N_i - 1$, N_i and $N_i + 1$ are shown, the lowest corresponding to commensurate filling. Compare the extension of the quenching interval of the variable J/U to the extension of the corresponding Mott insulator lobes in figure 3(a).

from which one easily calculates the corresponding superfluid fraction $f_s^{(\mathrm{ideal})}$ in terms of $\mathrm{d}E^{(\omega)}_{\mathrm{ideal}}(N)/\mathrm{d}\omega^2$. One can then set up a quenching factor Q defined as the ratio

$$Q \equiv \frac{f_s}{f_s^{(\mathrm{ideal})}} = \frac{\mathrm{d}E^{(\omega)}/\mathrm{d}\omega^2|_{\omega=0}}{\mathrm{d}E^{(\omega)}_{\mathrm{ideal}}/\mathrm{d}\omega^2|_{\omega=0}} = \left.\frac{\mathrm{d}E^{(\omega)}}{\mathrm{d}\omega^2}\right|_{\omega=0} \frac{M^2\omega_0^2}{4\pi^2 JN}.$$

If now one takes into account the relation between the cranking angular velocity and the 'twist' Θ used in ([17]), namely $\Theta = 2\pi\omega/\omega_0$, to express the quenching factor Q in terms of $\mathrm{d}E^{(\omega)}/\mathrm{d}\Theta^2$, one obtains the expression used there for the superfluid fraction.

5. Properties related to condensation

Equation (15) and its interpretation that full coherence of the superfluid current is restored only in the limit where only one of the natural orbitals is occupied suggests that further attention

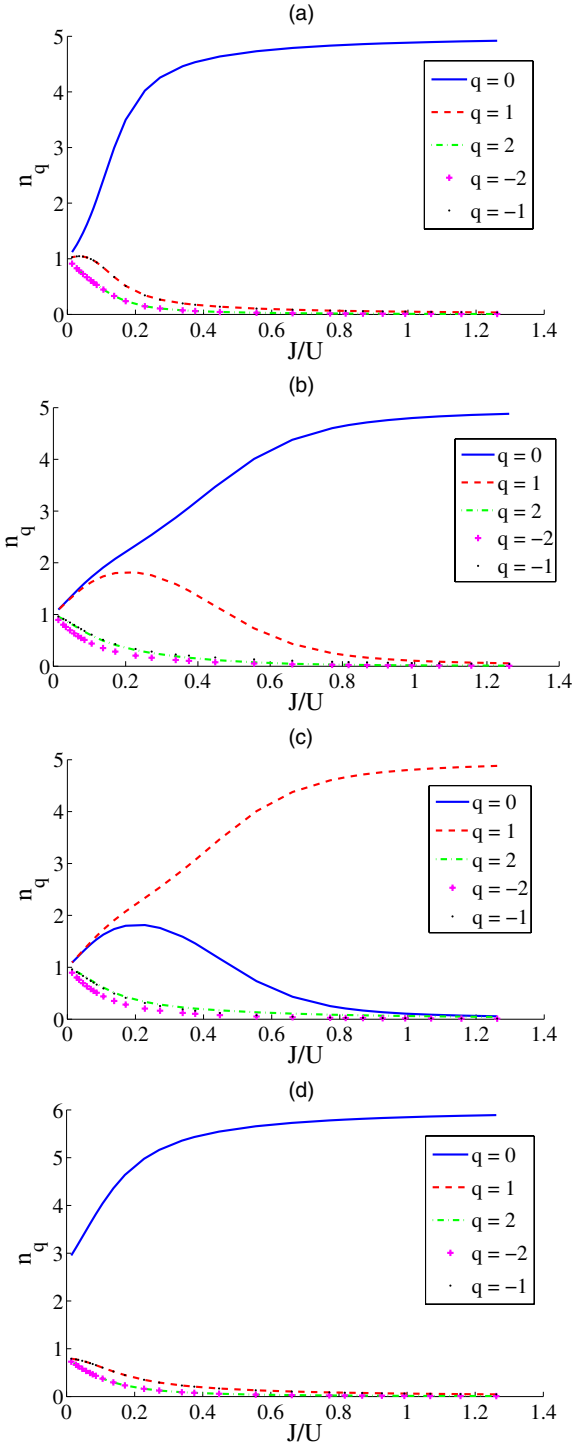

Figure 6. Eigenvalues of the reduced density matrix for $\Lambda = 0.06\epsilon_0$ and $M = 5$. In (a)–(c) the mean filling per site $N/M = 1$, while in (d), $N/M = 1.2$. In (a), $\omega = 0$ while in (b), $\omega = 0.48\omega_0$ and in (c), $\omega = 0.52\omega_0$, i.e. just before and after the single-particle level crossing at $\omega = 0.5\omega_0$. At $\omega = 0.5\omega_0$ there is a migration of population from the state with quasi-momentum $q = 0$ in (a) and (b) to the one with $q = 1$ in (c); (d) illustrates qualitative differences in the limit $J/U \to 0$ between the incommensurate and the commensurate situations.

should be given to the eigenvalues and eigenvectors of the one-body density matrix. In fact, their properties are related to the Penrose and Onsager criteria [20] for characterizing

Bose–Einstein condensation in systems of interacting bosons. It is defined in terms of the macroscopic occupation of a natural orbital, which then plays the role of 'condensate wavefunction' (see equation (20) and discussion on the spectral decomposition of the reduced density matrix in section (4)). Barring important limiting procedures which have to be used when dealing with extended systems, and notwithstanding non-existence theorems for Bose–Einstein condensation as a phase transition in one-dimensional systems [25], in the present case of fixed, finite number of bosons the behaviour of the natural orbital occupation numbers with the parameters of the model Hamiltonian is still revealing of condensation oriented one-body properties of the correlated many-boson state.

Typical behaviour for occupation numbers of the system's ground-state natural orbitals is shown in the plots of figures 6(a)–(c) for a situation with commensurate filling (the number of bosons N being an integer multiple of the number of sites in the array, M), and in figure 6(d) for an incommensurate case. In all cases the two-body interaction parameter has been fixed at $\Lambda = 0.06\epsilon_0$. Use of the larger value $\Lambda = 0.3\epsilon_0$, as in figures 4 and 5, gives however essentially identical results, reflecting the validity of the tight-binding approximation in this context. Since in the incommensurate case one may have to deal with different values of total quasi-momentum due to the ω-dependence of the Bloch energies, the two cases are better discussed separately.

We begin with the commensurate situation where, regardless of the values of ω, the ground state of the many-body system is always found in the subspace of total quasi-momentum $Q_T = 0$. As shown in figures 6(a)–(c), evaluated for the case $N = M$, in the extreme tight-binding limit $J \to 0$, one has a fully degenerate situation in which each of the orbitals has unit occupation, implying that the reduced one-body density is an *incoherent* superposition with equal weights of one body densities constructed from each of the first-band Bloch functions. This is in fact a consequence of the localization of each particle in one of the sites, achieved through probability amplitudes involving the (Wannier) *coherent* superposition of the Bloch functions. In the commensurate case with $\rho_0 = 1$, localization causes the two-body energy to vanish in the limit $J \to 0$. Increasing the effective hopping parameter J by lowering the barrier strength leads eventually to a situation in which the trace of the reduced one-body density is carried by essentially a single eigenvalue, the associated natural orbital being the Bloch state with lowest single-particle energy at the considered value of the cranking angular velocity ω. This implies that the spectral decomposition of the reduced one-body density essentially reduces to a single term, which corresponds to the underlying many-body state approaching the simple form of a product state in which all bosons are coherently delocalized in the collectively occupied Bloch wavefunction. Parts (b) and (c) of figure 6 illustrate the change of role of Bloch orbitals near the level crossings at $\omega = 0.5\omega_0$.

Figure 6(d) shows the evolution under increasing effective hopping parameter J of the eigenvalues of the reduced one-body density in the incommensurate case $N = 6$, $M = 5$ for $\omega = 0$. Unlike in the commensurate case, here one no longer has occupation number degeneracy for the natural orbitals at the extreme tight-binding limit $J \to 0$, but an occupation enhancement of the lowest Bloch state which in fact typically exceeds the contribution of the extranumerary boson, an effect which may be traced to the action of bosonic enhancement factors [24]. The delocalization process induced by hopping, associated with progressive dominance of a single Bloch state, is however maintained.

Finally, it is worth noting that, in all cases, the scale over which the transition to delocalization occurs, in terms of J/U coincides with that which may be associated with the extension of the Mott insulator lobes in the ground-state phase diagram (see figure 3), suggesting the connection of these two features.

5.1. Discussion

The relatively small values obtained for the superfluid fraction throughout the range of barrier strengths in which the delocalization transition takes place is perhaps not surprising if one keeps in mind that this range falls within the tight-binding domain in which the Bose–Hubbard model is an excellent approximation to the present treatment of the Hamiltonian (7), and that the potential barriers themselves constitute an important mechanism coupling the externally imposed rotation to the dynamics of the many-body system. From this point of view, the obtained values for the superfluid fraction based on the two-fluid model arise from a current, in the rotating frame of reference in which the lattice potential is at rest, that still manages to flow through the hindrance of the potential barriers.

There are two features of this current that deserve some remarks. First, the fact that in the present one-dimensional circular geometry it is independent of position on the circle (see equation (17)) is clearly a necessary consequence of stationarity, which in particular requires a time independent one-body density. Moreover, the restriction to the Bloch orbitals of the first band, together with the (modular) conservation of quasi-momentum by the Hamiltonian (7), imply the vanishing of mean field effects of the two-body force, thus causing the first-band Bloch states themselves to play the role of eigenstates of the reduced one-body density. From the one-body equation leading to them it follows that each of the individual square brackets in equation (17) vanishes for the numerical calculations reported here. It should be kept in mind, however, that this is just an artefact of the adopted truncation of the single particle basis, and not true in the general case in which, according to equation (17), only the appropriately weighted sum of them is independent of φ.

The second feature deserving comment is the fact that the current associated with the superfluid fraction is generally given as an incoherent sum of contributions associated with each of the populated eigenstates of the reduced one-body density. Thus, to the extent that it favours the occupation of a single such eigenstate, the delocalization transition associated with the closing of the Mott insulator lobes effectively promotes the complete coherence of the full current. In

the context of the calculations reported here, the effects of incoherence stem from the different values of the (φ-independent) contributions of the first-band Bloch states together with the respective occupation numbers. The special role played by the Bloch states is however also an artefact of the adopted truncation of the single-particle base. In general, further many-body dynamical effect will be encoded in the structure of the eigenstates of one-body density.

6. Conclusions

We presented a numerical study of properties of a small system of identical bosons in one-dimensional circular lattice undergoing rotation. The calculations were based on the diagonalization of the standard many-body Hamiltonian in the external lattice potential with contact two-body effective interactions truncating the involved single particle basis to the first-band Bloch states of the rotating lattice. With the appropriate scaling of the system parameters, results agree quantitatively with those obtained from the simple Bose–Hubbard model in the tight-binding limit, but will elsewhere incorporate additional effects (such as modified single-boson energy spacings and hopping effects other than nearest neighbours), subject to the limitations imposed by the adopted truncation (to the first band) of the single-particle orbitals.

Results obtained for a reinterpretation of the (grand-canonical) ground-state phase diagram in terms of 'separation energies' obtained by comparing ground-state energies of systems with different numbers of particles reproduce results of known grand-canonical calculations quantitatively even for a small lattice, including the 'reentrant behaviour' of the Mott insulator lobes characteristic of one-dimensional systems. The closing of the lobes is clearly associated with the delocalization of the bosons over the lattice which results from the progressive occupation of a single eigenstate of the one-body reduced density matrix.

Numerical results for ground-state superfluid fractions, obtained in the context of two-fluid phenomenology, link the closing of the Mott insulator lobes with increased coherence of a uniform, solenoidal single particle current associated with the intrinsic inertia of the superfluid fraction. This association can be formally extended to three-dimensional traps, also independently of assuming the existence of a condensed mode or any particular currents associated with it.

The value of the superfluid fraction remains small throughout the parameter domain associated with the transition, and grows monotonically saturating at the value 1 only with the complete smoothing out of the lattice. This suggests that the 'Mott-insulator to superfluid transition' may be a transition related rather to properties of coherence and delocalization, than to superfluidity in terms of propensities in the system to physical flow.

Acknowledgments

FP thanks Jonas Larson and Jani-Petri Martikainen for useful comments and discussions. Work has been supported by FAPESP and the Swedish Research Council (Vetenskapenrådet).

References

[1] Davis K B, Mewes M O, Andrews M R, van Druten N J, Durfee D S, Kurn D M and Ketterle W 1995 *Phys. Rev. Lett.* **75** 3969–73
[2] Anderson M H, Ensher J R, Matthews M R, Wieman C E and Cornell E A 1995 *Science* **269** 198
[3] Huang K 1996 *Bose–Einstein Condensation* ed A Griffin, D W Snoke and S Stringari (Cambridge: Cambridge University Press)
[4] Lieb E H, Seiringer R, Solovej J P and Yngvason J 2005 *The Mathematics of the Bose Gas and its Condensation* 1st edn (Basel: Birkhäuser)
[5] Pethick C J and Smith H 2008 *Bose–Einstein Condensation in Dilute Gases* 2nd edn (Cambridge: Cambridge University Press)
[6] Pitaevski L and Stringari S 2003 *Bose Einstein Condensation* (New York: Oxford University Press)
[7] de Toledo Piza A F R 2004 *Braz. J. Phys* **34** 1102–57
[8] Leggett A J 2006 *Quantum Liquids* (New York: Oxford University Press)
[9] Greiner M, Mandel O, Esslinger T, Hnsch T W and Bloch I 2001 *Nature* **415** 39–44
[10] Lieb E H, Seiringer R and Yngvason J 2002 *Phys. Rev.* B **66** 134529
[11] Amico L, Osterloh A and Cataliotti F 2005 *Phys. Rev. Lett.* **95** 063201
[12] Cooper N R and Hadzibabic Z 2010 *Phys. Rev. Lett.* **104** 030401
[13] Dubessy R, Liennard T, Pedri P and Perrin H 2012 *Phys. Rev.* A **86** 1
[14] Ryu C, Andersen M F, Clad P, Natarajan V, Helmerson K and Phillips W D 2007 *Phys. Rev. Lett.* **99** 260401
[15] Desbuquois R, Chomaz L, Yefsah T, Léonard J, Beugnon J, Weitenberg C and Dalibard J 2012 *Nature Phys.* **8** 645648
[16] Roth R and Burnett K 2003 *Phys. Rev.* A **68** 023604
[17] Roth R and Burnett K 2004 *Phys. Rev.* A **69** 021601
[18] da Cunha B R and de Oliveira M C 2006 *Int. J. Mod. Phys.* B **20** 1671
de Oliveira M C and da Cunha B R 2009 *Int. J. Mod. Phys.* B **23** 5867
[19] Fisher M P A, Weichman Peter B, Grinstein G and Fisher D S 1989 *Phys. Rev.* B **40** 546570
[20] Penrose O and Onsager L 1956 *Phys. Rev.* **104** 576–84
[21] Jaksch D, Bruder C, Cirac J I, Gardiner C W and Zoller P 1998 Cold bosonic atoms in optical lattices *Phys. Rev. Lett.* **81** 3108
[22] Kühner T D, White S R and Monien H 2000 *Phys. Rev.* B **61** 12474
[23] Pino M, Prior J and Clark S R 2013 *Phys. Status Solidi* b **250** 51
[24] de Toledo Piza A F R 2005 *Braz. J. Phys.* **35** 112–29
[25] Cazalilla M A, Citro R, Giamarchi T, Orignac E and Rigol M 2011 *Rev. Mod. Phys.* **83** 14051466
[26] Yukalov V I 2009 *Laser Phys.* **19** 1–110